



Experimental rig to estimate the coefficient of friction between tire and surface in airplane touchdown simulations

Chengwei Li and Liwei Zhan

Citation: [Review of Scientific Instruments](#) **86**, 085102 (2015); doi: 10.1063/1.4927681

View online: <http://dx.doi.org/10.1063/1.4927681>

View Table of Contents: <http://scitation.aip.org/content/aip/journal/rsi/86/8?ver=pdfcov>

Published by the [AIP Publishing](#)

Articles you may be interested in

[Toward the acoustical characterization of asphalt pavements: Analysis of the tire/road sound from a porous surface](#)

J. Acoust. Soc. Am. **125**, 5 (2009); 10.1121/1.3025911

[System for measuring the coordinates of tire surfaces in transient conditions when rolling over obstacles: Description of the system and performance analysis](#)

Rev. Sci. Instrum. **79**, 065105 (2008); 10.1063/1.2932339

[Experimental design to maximize information](#)

AIP Conf. Proc. **568**, 192 (2001); 10.1063/1.1381884

[Transient behavior of the moments of a stochastic differential equation with two random coefficients](#)

AIP Conf. Proc. **519**, 332 (2000); 10.1063/1.1291576

[Nonlinear features in the dynamics of an impact-friction oscillator](#)

AIP Conf. Proc. **502**, 469 (2000); 10.1063/1.1302423

An advertisement for Oxford Instruments. On the left, there is a circular inset image showing a man with glasses and a beard, wearing a lab coat and gloves, working with scientific equipment. To his right, the text reads "'On the way to a graphene spin field effect transistor' by Prof. Barbaros and the Özyilmaz Group at National University of Singapore". At the top right is the Oxford Instruments logo with the tagline "The Business of Science". Below the logo is a call-to-action button that says "Download a FREE application note".

'On the way to a graphene spin field effect transistor'

by Prof. Barbaros and the Özyilmaz Group at National University of Singapore

Download a FREE application note

Experimental rig to estimate the coefficient of friction between tire and surface in airplane touchdown simulations

Chengwei Li and Liwei Zhan

School of Electrical Engineering and Automation, Harbin Institute of Technology,
Harbin 150001, People's Republic of China

(Received 28 April 2015; accepted 20 July 2015; published online 4 August 2015)

To estimate the coefficient of friction between tire and runway surface during airplane touchdowns, we designed an experimental rig to simulate such events and to record the impact and friction forces being executed. Because of noise in the measured signals, we developed a filtering method that is based on the ensemble empirical mode decomposition and the bandwidth of probability density function of each intrinsic mode function to extract friction and impact force signals. We can quantify the coefficient of friction by calculating the maximum values of the filtered force signals. Signal measurements are recorded for different drop heights and tire rotational speeds, and the corresponding coefficient of friction is calculated. The result shows that the values of the coefficient of friction change only slightly. The random noise and experimental artifact are the major reason of the change. © 2015 AIP Publishing LLC. [<http://dx.doi.org/10.1063/1.4927681>]

I. INTRODUCTION

Friction between two bodies in contact is a complex process. Computational models do not capture the true essence of friction in real situations.^{1,2} At present, experimental research mainly focuses on investigating the coefficient of friction.^{3,4} However, there are few studies on the coefficient of friction of airplane tires.⁵ During touchdowns, the coefficient of friction of a tire depends on many factors such as the materials and time in contact, the moving velocity, material surface conditions, and so on.⁶ To simulate these events and to estimate the coefficient of friction between tire and runway surfaces, we designed an experimental rig that can simulate various landing scenarios and designed a platform to measure the force of impact and friction between tire and runway surface. Whereas, drop testing with landing gear is different^{7–9} and the main focus with this device is on coefficient of friction of a tire.

Noise is inevitable during the measurement of the forces involved. To improve the quality of signals, it is necessary to remove noise from the measured signals. Wavelet filtering has been the dominant technique for many years.¹⁰ Nevertheless, noise does affect quantifying wavelet coefficients. The wavelet thresholding method addresses this issue and enables de-noising of the signals.¹¹ The drawback is that the wavelet basis functions are pre-defined and more importantly the analysis is not adaptive in nature. The empirical mode decomposition (EMD), first introduced by Huang,¹² has been used to analyze the signal data derived from non-stationary and non-linear systems. This expansion enables signals to be decomposed into a set of “well-behaved” oscillatory functions, referred to as the intrinsic-mode functions (IMFs). The powerful adaptive EMD tool has received much attention with applications in signal filtering.^{13–15} However, EMD is unable to accurately provide a physical meaning of the signal because of mode mixing. To overcome this drawback, Wu and Huang have proposed the ensemble EMD (EEMD).¹⁶ This method offers a noise-assisted analysis and adds white noise with a

uniform frequency distribution into EMD to eliminate mode mixing.

In this paper, we propose a filtering method, which employs the EEMD and bandwidth of Probability Density Function (PDF) for each IMF for signal de-noising. PDF contains information about the amplitude and frequency of the signal. Bandwidth, an important parameter of PDF, can represent information of PDF. We can consider bandwidth as threshold value. This method is effective in removing noise, the results of which are to be compared with those from wavelet filtering. We measure the coefficient of friction under various conditions specified by drop height and tire rotation speed. The measurement result shows that the coefficient of friction changes very little. We discuss the reason of the variation. The rest of the paper is organized as follows. Section II describes the measurement system, Section III the signal filtering, Section IV the coefficient of friction, and Section V present conclusions.

II. MEASUREMENT SYSTEM

A. Structure of the measurement assembly

This measurement assembly (Fig. 1) is a vertical drop test system consisting of a drop mechanism, an impact platform, support fixtures, frame, and tire turning system.

B. Working principle

During the measurement procedure, the drop mechanism is first lifted to a specified height. The tire is then spun using a rotary motor to a specified angular speed for the drop test. Once conditions are met, drop mechanism falls along frame and hits with turning tire. The impact force and friction are measured between tire and surface as the impact platform engages with the tire. The drop mechanism simulates the weight of the airplane. The angle of landing attack is simulated by the speed of the vertical drop and the angular speed of the tire. The turning tire simulates the aircraft speed at touchdown.

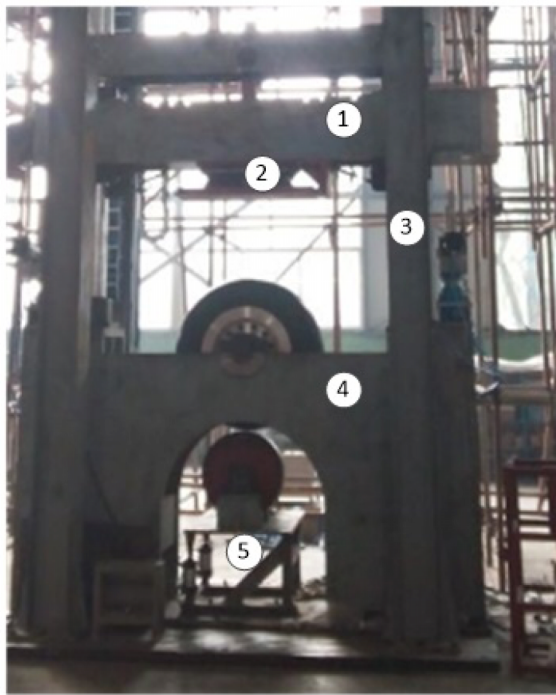


FIG. 1. Photo of the measurement assembly (1: drop mechanism; 2: impact platform; 3: frame; 4: support fixtures; 5: tire turning system).

C. Impact platform

In this experimental rig, an important design part is the impact platform that is composed of two subsystems (Fig. 2): one measures the impact force (framed in solid line) and the other the friction force (framed in dashed line). The impact subsystem includes three layers; three piezoelectricity force sensors in the first and second layers are used to measure the impact force components between tire and surface. The third layer is the impact platform, which is able to move along the slide-way direction between the second and third layers. The force of friction is measured using two piezoelectricity force sensors. Figure 3 gives a photo of the actual device.

III. SIGNAL FILTERING

A. Filtering principle

The main idea of the proposed filtering method is that the force signal modes often concentrates around the last IMFs and noise signal modes concentrates around the first IMFs.

The amplitude of the oscillations of the last IMFs is smaller than that of the first IMFs. It is difficult to select the relevant mode between the force signal modes and noise signal modes. Nevertheless, this problem can be tackled using the proposed method. The PDF contains information of the amplitude and frequency of the signal. Bandwidth is an important parameter of the PDF. We employ bandwidth to select the modes that correspond to the desired signal, noise, or both. To suppress mode mixing, the EEMD is used during filtering.

B. EMD algorithm

In our study, the EMD algorithm uses the follow steps:¹²

- (1) Extract all the extrema (maxima and minima) of the signal, $x(t)$.
- (2) Identify the upper and lower envelope using the cubic spline interpolation of the extrema point developed in step (1).
- (3) Calculate the mean function of the upper and lower envelope, $m_1(t)$.
- (4) Calculate the difference signal $d_1(t) = x(t) - m_1(t)$.
- (5) If $d_1(t)$ has a zero-mean, then the iteration is stopped and $d_1(t)$ is an IMF1, which we denoted by $c_1(t)$; otherwise, go to step (1).
- (6) Let $r(t) = x(t) - c_1(t)$.
- (7) If $r(t)$ has at least two extrema, then repeat steps (1)–(6) stopping if the final residual signal $r(t)$ is a monotonic function.

Ultimately, we obtain a residue $r(t)$ and a set of IMFs, $\{c_1(t), \dots, c_n(t)\}$. The original signal can be represented as

$$x(t) = \sum_{i=1}^n c_i(t) + r(t). \quad (1)$$

C. EEMD algorithm

In the reference,¹⁶ the EEMD algorithm has the following description:

- (1) Add a white noise series $n(t)$ to the targeted signal $x_1(t)$, $x_2(t) = x_1(t) + n(t)$.
- (2) Decompose signal $x_2(t)$ into a set of IMFs using the EMD algorithm.
- (3) Repeat steps 1 and 2 with different white noise series in each trial, to obtain the IMFs $c_{ij}(t)$, where i is the iteration number and j is the mode.

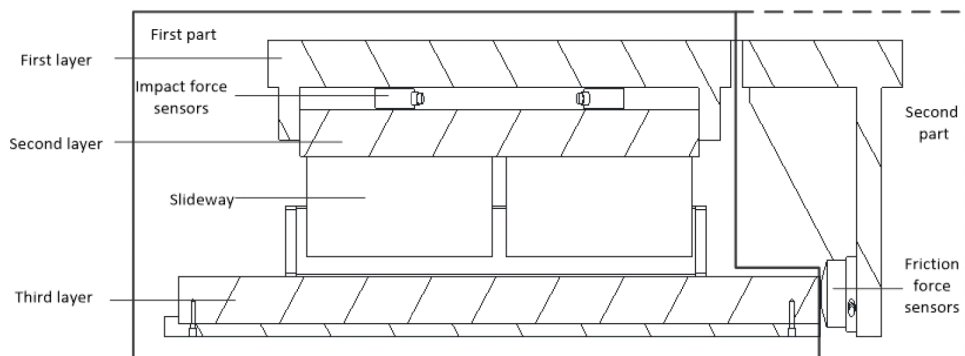


FIG. 2. Cross-sectional profile of the impact platform system.



FIG. 3. Photo of impact platform system showing various components (1: impact force sensors; 2: slide; 3: test platform; 4: friction force sensors).

TABLE I. The optimal bandwidth of each IMF.

IMF	1	2	3	4	5	6	7	8	9	10	11
h_{opt}	0.0113	0.0099	0.0082	0.0056	0.0041	0.0048	0.0052	0.0081	0.0117	0.0127	0.0736

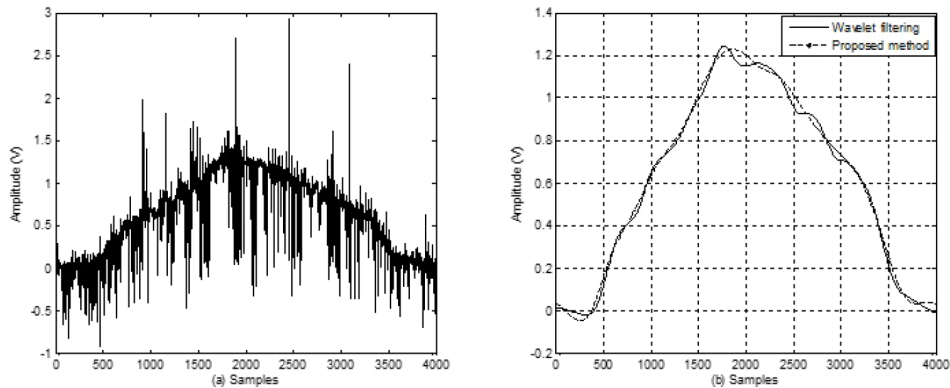


FIG. 4. Filtering of the signal for the friction force: (a) is the original signal and (b) gives the results obtained using the proposed filtering method and wavelet filtering.

- (4) Estimate the means of the corresponding IMFs for the decompositions as desired output,

$$c_j(t) = \frac{1}{N} \sum_{i=1}^N c_{ij}(t). \quad (2)$$

D. Kernel density estimation

Parzen introduced the kernel density estimation.¹⁷ This is a non-parameter method to estimate PDF of a data set and has been widely used in signal processing.^{18,19} The estimated PDF, denoted $\hat{f}(x)$, can be expressed as a sum,

$$\hat{f}(x) = (nh)^{-1} \sum_{i=1}^n K_h(x - X_i) \quad (3)$$

where h is the bandwidth of the PDF and $K_h(u) = K(u/h)$. Bandwidth h plays an important role in the estimation PDF; if h is too small, $\hat{f}(x)$ will be steep, and if h is too big, $\hat{f}(x)$ will be over-smooth. Here, we employ the mean-integrated-squared error (MISE)²⁰ to estimate the unknown PDF of the data set. MISE is defined by

$$\begin{aligned} \text{MISE} &= \int E\{\hat{f}_h(x) - f(x)\}^2 dx \\ &\approx \frac{1}{nh} R(K) + \frac{h^4}{4} [\mu_2(K)]^2 R(f''), \end{aligned} \quad (4)$$

where $R(K) = \int K(z)^2 dz$, $\mu_2(K) = \int z^2 K(z) dz$, $R(f'') = \int (f''(x))^2 dx$, and $f(x)$ is the real PDF. The asymptotic MISE is defined by

$$\text{AMISE} = \frac{1}{nh} R(K) + \frac{h^4}{4} [\mu_2(K)]^2 R(f''). \quad (5)$$

Setting $\frac{d\text{AMISE}}{dh} = 0$, we obtain the optimal bandwidth

$$h_{opt} = \left[\frac{R(K)}{[\mu_2(K)]^2 R(f'') n} \right]^{0.2}, \quad (6)$$

which contains the real PDF and the second-order derivative. This introduces error for the estimated PDF. To reduce this error, $R(K)/nh^5$ is brought into the expression for $R(f'')$.

$$R(f'') = R(\hat{f}'') - \frac{R(K)}{nh^5} \quad (7)$$

and hence the optimal bandwidth h_{opt} becomes

$$h_{opt} = \left[\frac{R(K)}{[\mu_2(K)]^2 (R(\hat{f}'') - \frac{R(K)}{nh^5}) n} \right]^{\frac{1}{5}}. \quad (8)$$

We chose a smooth Gaussian kernel to estimate PDF. In Eq. (8), parameter h is unknown. Here, we use Solve-the-Equation²¹ to solve for the optimal bandwidth, which is of

order

$$F(h) = \left[\frac{R(K)}{[\mu_2(K)]^2 \left(R(\hat{f}'') - \frac{R(K)}{nh^5} \right) n} \right]^{\frac{1}{5}}. \quad (9)$$

Algorithm: Solve-the-Equation.

- Calculate $h_1 = F(h_0)$, $h_0 = 1.06\sigma n^{-1/5}$.
- While $|h_1 - h_0| > \varepsilon$; here ε is a minimum.
- Set $h_0 = h_1$.
- Repeat step (a).
- Set $h_1 = (h_0 + h_1)/2$.

Ultimately, we obtain an optimal bandwidth $h_{opt} = h_1$ and are able to calculate an optimal estimated PDF using norm kernel function and h_{opt} .

E. Filtering method

To find the relevant mode, a signal $y(t)$ is first decomposed into IMFs using the EEMD, then the PDF of each IMF is estimated, and finally the optimal bandwidth h_{opt} is calculated. The PDF can represent information of IMF. From the first IMF to the last IMF, the optimal bandwidth of PDF of noise becomes increasingly smaller. When the bandwidth of an IMF suddenly becomes big, this IMF is the mode of the pure signal. We can distinguish the modes for noise and pure signal using the bandwidth. The filtering steps are as follows:

- A signal is decomposed into a set of IMFs using EEMD.
- The PDF of the IMFs is estimated and optimal bandwidth h_{opt} is calculated.
- The relevant mode k_{th} , the index of mode, is identified from the optimal bandwidth h_{opt} ,

$$k_{th} = \operatorname{argmin}\{h_{opt}\} + 1. \quad (10)$$

- Set the IMFs to zero before k_{th} and reconstruct the signal

$$y(t) = \sum_{i=k_{th}}^n IMF_i + r_n(t). \quad (11)$$

F. Measured signal filtering

Here, we employ the above filtering method to filter the friction signal (drop height of 330 mm and tire rotation speed of 150 rps). Table I is the value of optimal bandwidth. The

results of filtering are compared with that for wavelet denoising (Fig. 4) and they show that these methods are capable of extracting signal information. The proposed filtering method however produces a very smooth curve and shows a definite peak in the signal.

IV. COEFFICIENT OF FRICTION

To remove noise from the measured signal, we must filter the signal. Solving the coefficient of friction is difficult because modeling the situation is not easy. Photos are given of the marks left on the impact platform and wear on the tire (Fig. 5).

To quantify the coefficient of friction between tire and surface, we have performed many experiments. The coefficient of friction is calculated using the expression

$$\mu = \frac{f}{F_N}, \quad (12)$$

where F_N is the tire impact force (pressure) and f is the friction force. To ensure the result of reliable measurements, the bandwidth of the selected sensor is 40 KHz after estimating the natural frequency of main research object (the test platform in Figure 3). Here, the natural frequency of test platform is about 14 KHz. Measured signals are synchronously recorded with sampling frequency 110 KHz. Technical data of the impact force device, which consists of five piezoelectric force sensors and charge amplifiers, are listed in Table II.

Sensors 1, 2, and 3 were used to measure the impact force, and the others are used to measure friction. We calculated the force using

$$F = U/SG, \quad (13)$$

where F is the component of the force, U the measured voltage, S the sensitivity of sensor, and G the gain of the charge amplifier. After the measured signal is filtered, we calculated the maximum of each sensor signal to obtain the impact force and friction force. Table III lists the results for the force of impact and friction under different scenarios for drop height and rotation speed.

In plotting the coefficient of friction for different drop heights (Fig. 6), we observe that the values of coefficient of friction are relatively stable (the variation is 0.01). Given the theoretical assumptions, the coefficient of friction is independent of height, nevertheless deviations are expected. The main reason is that the noise and other experimental artifact,



FIG. 5. Photos showing marks on the impact platform and the tire.

TABLE II. Parameter of sensors and charge amplifier.

Sensor number	Range (KN)	Sensitivity (pC/N)	Bandwidth of sensor (KHz)	Gain of charge amplifier (mV/pC)
1	300	2.081	40	0.05
2	300	2.062	40	0.05
3	300	2.098	40	0.05
4	300	2.094	40	0.05
5	300	2.078	40	0.05

TABLE III. Experimental results for force of impact and friction. The data in italics indicate friction force (KN) data, and others indicate impact force (KN) data.

Drop height (mm)	Tire rotational speed (RPS)					
	150	200	250	150	200	250
330	62.652	23.4723	64.5932	24.2483	67.034	25.2182
430	67.6453	25.2182	69.4435	25.9580	72.4514	27.1584
530	70.86	26.158	74.9353	27.8160	75.3495	28.1280
630	74.4084	27.5460	78.3758	28.6759	77.8851	29.0979
729	76.5189	28.7099	79.8225	29.9175	83.7168	31.4859

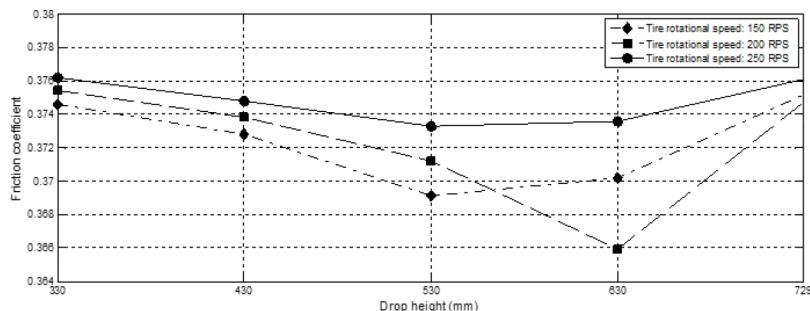


FIG. 6. Dependence of coefficient of friction on drop height.

which are random in the experiment, influence the measuring result.

V. CONCLUSION

In this paper, an experimental device to simulate airplane touchdowns was described and used in experiments to measure the force of impact and friction between tire and runway surface. In the presence of noise, a method based on the EEMD and PDF bandwidth for each IMF was proposed and used to extract the force signals. The results of this method were compared with those using wavelet filtering and demonstrated superior performance by filtering out noise. To objectively quantify the coefficient of friction between tire and surface, various forces of impact and friction were measured by varying drop height and rotation speed of the tire from which the coefficient of friction can then be calculated. Measurement results for all touchdown scenarios show that coefficient of friction only changes slightly, and the variation reason is analyzed.

¹E. J. Berger, "Friction modeling for dynamic system simulation," *Appl. Mech. Rev.* **55**(6), 535 (2002).

²J. Swevers, F. Al-Bender, C. G. Ganseman *et al.*, "An integrated friction model structure with improved presliding behavior for accurate friction compensation," *IEEE Trans. Autom. Control* **45**(4), 675–686 (2000).

³Y. L. Lin, J. G. Qin, R. Chen *et al.*, "A technique for measuring dynamic friction coefficient under impact loading," *Rev. Sci. Instrum.* **85**(9), 094501 (2014).

⁴E. Brueschke and B. Eckman, "Device for the measurement of friction at ultrahigh vacuum," *Rev. Sci. Instrum.* **34**(9), 978–980 (1963).

⁵A. Norheim, N. K. Sinha, and T. J. Yagera, "Effects of the structure and properties of ice and snow on the friction of aircraft tyres on movement area surfaces," *Tribol. Int.* **34**(9), 617–623 (2001).

⁶M. K. Ramasubramanian and S. D. Jackson, "A friction sensor for real-time measurement of friction coefficient on moving flexible surfaces," in *Proceedings of IEEE Sensors* (IEEE, 2003), Vol. 1, pp. 152–157.

⁷C. C. Daughetee, "Drop testing naval aircraft and the VSD landing gear dynamic test facility," AIAA Paper 74-343, 1974.

⁸I. Ross and R. Edson, "Application of active control landing gear technology to the A-10 aircraft," NASA Report CR 166104, 1982.

⁹J. P. Kong, Y. S. Lee, J. D. Han, and O. S. Ahn, "Drop impact analysis of smart unmanned aerial vehicle (SUAV) landing gear and comparison with experimental data," *Materialwiss. Werkstofftech.* **40**(3), 192–197 (2009).

¹⁰V. D. Hoang, "Wavelet-based spectral analysis," *TrAC, Trends Anal. Chem.* **62**, 144–153 (2014).

¹¹D. L. Donoho, "De-noising by soft-thresholding," *IEEE Trans. Inf. Theory* **41**, 613–627 (1995).

- ¹²N. E. Huang, Z. Shen, S. R. Long, M. C. Wu, H. H. Shih, Q. Zheng, N. C. Yen, C. C. Tung, and H. H. Liu, "The empirical mode decomposition and the Hilbert spectrum for nonlinear and non-stationary time series analysis," *Proc. R. Soc. A: Math. Phys. Eng. Sci.* **454**, 903–995 (1998).
- ¹³K. Khaldi, M. Turki-Hadj Alouane, and A. O. Boudraa, "Speech denoising by adaptive weighted average filtering in the EMD framework," in *2nd International Conference on Signals, Circuits and Systems (SCS)*, 2008.
- ¹⁴A. O. Boudraa and J. C. Cexus, "EMD-based signal filtering," *IEEE Trans. Instrum. Meas.* **56**, 2196–2202 (2007).
- ¹⁵A. Komaty, A. Boudraa, and D. Dare, "Emd-based filtering using the Hausdorff distance," in *IEEE International Symposium on Signal Processing and Information Technology (ISSPIT)*, 2012.
- ¹⁶Z. Wu and N. E. Huang, "Ensemble empirical mode decomposition: A noise-assisted data analysis method," *Adv. Adapt. Data Anal.* **01**, 1–41 (2009).
- ¹⁷E. Parzen, "On estimation of a probability density function and mode," *Ann. Math. Stat.* **33**, 1065–1076 (1962).
- ¹⁸K. G. Margaritis and P. D. Michailidis, "Parallel computing of kernel density estimation with different multi-core programming models," in *Euromicro International Conference on Parallel, Distributed, and Network-Based Processing* (IEEE, 2013), pp. 77–85.
- ¹⁹X. Xu, Z. Yan, and S. Xu, "Estimating wind speed probability distribution by diffusion-based kernel density method," *Electr. Power Syst. Res.* **121**, 28–37 (2015).
- ²⁰B. A. Turlach, *Bandwidth Selection in Kernel Density Estimation: A Review* (Université catholique de Louvain, Louvain-la-Neuve, 1993).
- ²¹L. A. Alexandre, "A solve-the-equation approach for unidimensional data kernel bandwidth selection," available online at: <http://www.di.ubi.pt/~lfbba/entnetsPubs/bandwidth.pdf>, 2008.